

Original Research Article**Far-Infrared Spectra of the Alloy of
Germanium-Antimony-Tellurium
in the Glassy and Crystalline State****ABSTRACT**

Far-infrared spectra of a germanium-antimony-tellurium alloy in the glassy and crystalline states have been measured and analyzed in the frequency range 20–400 cm⁻¹ at room temperature. The absorption in this range is due to the phonon modes of the structural units of crystalline and correlated librational vibrations (boson peak) of glassy alloy, which precede the appearance of relaxation dynamics. The vibrational assignments of various absorption bands and the differences revealed in the spectra will make it possible to more confidently elucidate the possible molecular mechanism of the crystal-to-amorphous transition in other chalcogenide alloys. New details of the crystal-to-amorphous transition scenario are suggested.

Keywords: far-infrared spectra, phonons, boson peak, chalcogenide, phase transition.

1. INTRODUCTION

Phase-change materials (PCMs) based on chalcogenide alloys are of great technological importance due to their ability to undergo on being heated a fast and reversible transition between the amorphous and crystalline phases [1, 2]. This property is exploited in rewritable optical media and electronic nonvolatile memory, which are based on the strong optical and electronic contrast between the two phases [3].

Te-containing chalcogenides such as the Ge-Sb-Te ternary alloy system usually abbreviated as GST has been known to satisfy material requirements for PCM. However, although GST s are already in use for the rewritable compact discs and digital versatile discs and their commercial application in electronic non-volatile memory devices is expected in the near future as well; neither the local structure of material nor the change in the structure during the phase transition is well established. Several details of the electronic structure GST, which are supposed to control the transport properties and the switching mechanism, are still a matter of debate. One are suggest that the strong optical and electronic contrast between the amorphous and crystalline phases GST system relate with a change in the coordination numbers [4], others with a change of bonding upon crystallization [5] or with a

high concentration of defects [6] and Peierls-distortion in an octahedral environment of Ge atoms [7].

In studies of the local atomic structure and dynamics of GST now uses the most advanced techniques such as the extended x-ray absorption fine structure (EXAFS) spectroscopy and spectroscopy of neutron scattering and Raman scattering (RS). Interestingly, the infrared (IR) spectroscopy is rarely used [8], and we do not know the IR absorption spectra of GST in the frequency range of RS-spectrum, which is based conclusions about the molecular mechanism of the phase transition in this system.

Infrared absorption of solids can provide useful information about the lattice vibrational density of solids and structure of solids. The vibrations that contribute to IR absorption yield the most direct structural information since their frequencies are determined primarily by nearest interactions and thus relative IR activity by local molecular symmetry. The IR spectroscopy is one of the most often used spectroscopic tools for the study of the crystals and amorphous materials (including chalcogenide) [9]. Its use for studying the structure of short- range order and of the dynamics of individual structural units of GST would be quite natural. Especially at low frequencies, where manifest multiphonon absorption in groups of the short- range order, lattice absorption in the crystal and disorder-induced absorption in glasses ("boson peak" by RS-spectroscopy terminology [10]).

However, out of the optical properties of the GST system is known only that they have a high transparency in the infrared range from edge of the electronic absorption up to the multiphonon edge near 20 microns. But recently in the mid-infrared region spectrophotometry was used to measure the transmittance of selected materials from this system [11]. The experimental data were successfully

50 interpreted in terms of Drude-type plasma of free carriers and it was found that the main increase of
51 optical constants occurs in the far-infrared domain. Consequently, the far-infrared spectroscopy
52 appears to be convenient experimental method to study directly the structure and dynamics of the
53 system GST. This is also evidenced by the results of the comparative study and analysis of the time-
54 domain terahertz (THz) spectra of four different GST compounds in whose spectra observed a
55 phonon mode and a contribution of free charge carriers at range of 10-80 cm^{-1} [12].

56 The aim of the present study was to obtain the IR transmission spectra of polycrystalline and glassy
57 material of the GST system containing 15 at % germanium, 15 at % antimony and 70 at % tellurium
58 (further $\text{Ge}_{15}\text{Sb}_{15}\text{Te}_{70}$) in the region 20-400 cm^{-1} , to analyze them on the basis of calculation and of
59 the literature data, and to find the relationship between the parameters of the far-infrared spectra and
60 the molecular characteristics of $\text{Ge}_{15}\text{Sb}_{15}\text{Te}_{70}$. The results are interpreted in terms of the vibrations of
61 the isolated molecular units of investigated alloy. Detailed comparisons of obtained spectra has
62 shown that glassy $\text{Ge}_{15}\text{Sb}_{15}\text{Te}_{70}$ exhibits a characteristic extreme far-infrared absorption as result of
63 phonon coupling to modes which are not active in the corresponding crystalline counterpart material.
64 The made vibrational assignments of various absorption bands and the revealed differences in the
65 spectra will allow more confidently specify the possible molecular mechanism of the crystal-to-
66 amorphous transition in GST alloys.

67

68 2. MATERIAL AND METHODS / EXPERIMENTAL DETAILS /

69

70 Melt quench technique using elemental Ge, Sb and Te with 5N purity has been used for alloy
71 preparation of $\text{Ge}_{15}\text{Sb}_{15}\text{Te}_{70}$ glassy samples. The materials were weighed according to their atomic
72 weight percentages and sealed in evacuated ($\sim 10^{-3}$ Pa) quartz ampoules. The sealed ampoules were
73 kept inside a furnace, where the temperature was increased up to 950 $^{\circ}\text{C}$ at a heating rate of 3-4 $^{\circ}\text{C}$
74 min^{-1} . The ampoules were frequently rocked for 20 h to make the melt homogeneous. The melts were
75 rapidly cooled inside the furnace. The amorphous nature of the obtained glasses was confirmed by
76 the X-ray powder diffraction method [13]. The bulk samples were characterized using energy
77 dispersive X-ray spectroscopy for the analysis of compositions. To obtain polycrystalline samples, the
78 bulk samples were annealed in inert atmosphere for 120 min at temperature about 20 $^{\circ}\text{C}$ above the
79 temperature of amorphous - *fcc* phase transition determined by differential scanning calorimetry.

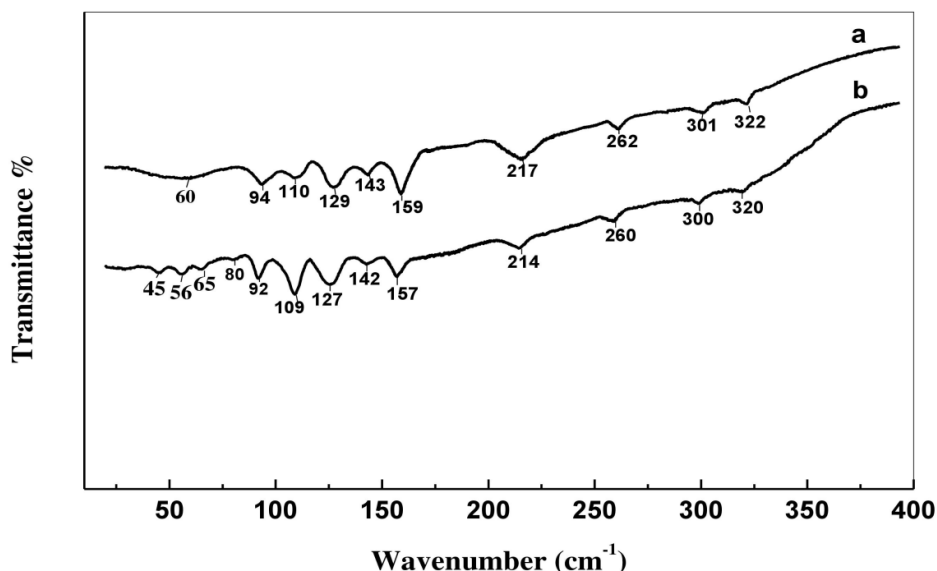
80 The far-IR absorption measurements were carried out in spectral range 20-400 cm^{-1} at room
81 temperature. Far-infrared spectra were obtained on two spectrometers. A spectrometer designed at
82 the Leningrad State University was used in the frequency range from 20 to 150 cm^{-1} . The spectra in
83 the range 150 to 400 cm^{-1} were recorded using Hitachi FIS-21 (Japan) spectrometer. The resolution
84 at a signal-to-noise ratio of the order of 100 was equal to 1 to 2 cm^{-1} . The location of the spectral
85 bands at their maxima was determined to within 1 - 2 cm^{-1} . All the measurements were carried out
86 using the polyethylene pellet method. The glassy and polycrystalline samples were thoroughly ground
87 to an average size of 10-15 μm ; grinding was performed in dry argon to exclude surface oxidation.
88 The pellets were made by mixing 2 mg sample with 200 mg of spectroscopic grade polyethylene and
89 pressed into pellets using hydraulic press (10 tons cm^{-2} for 5 min under vacuum). To take account of
90 polyethylene absorption, the spectrum of polyethylene was used as reference spectrum. The sample
91 spectrum was divided by the reference spectrum to nullify the polyethylene absorption.

92

93 3. RESULTS AND DISCUSSION

94

95 Figure shows the far-IR transmission spectra of polycrystalline and glassy material of GST of the
96 composition $\text{Ge}_{15}\text{Sb}_{15}\text{Te}_{70}$ in the region 20 - 400 cm^{-1} . The recorded spectra have the form of the
97 almost structureless plateau on which background can pick out several peaks of the overlapping
98 absorption bands. The most notable ones are at 60 cm^{-1} , 94 cm^{-1} , 110 cm^{-1} , 129 cm^{-1} , 159 cm^{-1} and
99 217 cm^{-1} in the spectrum of glassy and at 45 cm^{-1} , 56 cm^{-1} , 65 cm^{-1} , 92 cm^{-1} , 109 cm^{-1} , 127 cm^{-1} ,
100 157 cm^{-1} and 214 cm^{-1} in the spectrum of polycrystalline material.



101

102 . Figure 1. Far-infrared spectra of GST material of composition $\text{Ge}_{15}\text{Sb}_{15}\text{Te}_{70}$ in the
103 amorphous (a) and the crystalline (b) state.

104 The tentative assignments of these bands were carried out on the basis of calculations in which the
105 GTS alloy is considered as a spatial three-dimensional polymer. Its structure has been expressed in
106 the form of the two covalently constructed structural units - of areas of short-range order- tetrahedral
107 “molecules” of GeTe_4 and pyramidal “molecules” of SbTe_3 . The validity of this approach follows from
108 the close relationship between the vibrational spectra of molecules or molecular ions and the
109 vibrational spectra of glass-like solids containing the same or analogous structural groups in the form
110 of areas of short-range order.

111 The GeTe_4 molecule has 5 atoms and thus supports 15 modes of motion, including 3 pure rotations
112 and 3 pure translations. The T_d symmetry of the GeTe_4 molecule leads to 6 zone- center modes
113 following the decomposition in standard notation [14]:

114 $\Gamma(T_d) = A_1 + E + F_1 + 3F_2$,

115 where F_1 corresponds to a pure rotation (noted as R in the literature), and one of the F_2 is a pure
116 translation (noted as T). R and T modes are related to the external modes. The modes derived from
117 the tetrahedral A_1 , E and $2F_2$ modes are usually named as ν_1 , ν_2 , ν_3 and ν_4 , respectively, and are
118 considered as internal modes of the GeTe_4 tetrahedra in $\text{Ge}_{15}\text{Sb}_{15}\text{Te}_{70}$.

119 The modes which predicts a group theory for a tetrahedral symmetry and the calculated phonon
120 frequencies at the $\Gamma(T_d)$ -point are reported in Table 1. They are attributed as shown in Table 1 below
121 in accordance with the assignments of the GeI_4 molecular vibrations [15, 16].

122 **Table 1. Normal vibrational modes of the GeI_4 and GeTe_4 tetrahedra.**

123 **From the spectrum of a Ge-Sb-Te alloy composition $\text{Ge}_{15}\text{Sb}_{15}\text{Te}_{70}$.**

substance	Normal vibrational mode (cm^{-1}) [*]					
	ν_1	ν_2	ν_3	ν_4	ν_R	ν_T
GeI_4	159	60	264	80	56 [19]	-

GeTe ₄	125	87	209	78	60	55
Ge ₁₅ Sb ₁₅ Te ₇₀	127	92	214	80	65	60

124 v1 and v3 – the stretching modes for symmetric and antisymmetric vibrations,
 125 respectively;
 126 v2 and v4 – bending modes for symmetric and antisymmetric vibrations,
 127 respectively;
 128 vR and vT- external modes for pure rotation and pure translation, respectively.

129 We can use the analogy between modes of the GeTe₄ and the GeI₄ tetrahedra since the mass ratio of
 130 germanium tetraiodide is very similar to germanium tetratelluride and therefore can expect a
 131 correspondence in the respective frequencies.

132 Although only the v3 and v4 modes are infrared active in tetrahedral GeX₄ molecules, it is expected
 133 that all the fundamental modes appear in infrared absorption spectra because of breakdown of
 134 selection rules in polycrystalline and glassy materials. In addition the structure of crystalline GST is
 135 only “rock salt like” [1].

136 The SbTe₃ molecule crystallizes in a structure with symmetry C_{3v}. There are four atoms per unit cell
 137 and consequently SbTe₃ exhibits 12 phonon modes, including external R and T modes for each
 138 wavevector K. Group theoretical analysis yields for K = 0 the following reduction: $\Gamma_{tot}(C_{3v}) = 2A_{1g}$
 139 $+2A_{1u} + 2E_g + 2E_u$, which splits into acoustical modes and IR- or

140 Raman-active optical modes as follows: $\Gamma_{acoustical} = A_{1u} + E_u$, $\Gamma_{Raman} = 2A_{1g} + 2E_g$ and $\Gamma_{IR} = A_{1u} + E_u$, where
 141 one of the A_{1u} corresponds to a pure rotation and one of the E_u is a pure translation. Following the
 142 spectroscopic notation, the stretching modes are designated by v1 and v3 for the totally symmetric
 143 and the antisymmetric (double-degenerate) vibrations, respectively. Analogously, the bending modes
 144 correspond to v2 (A₁) and v₄ (E). All four vibrations are both infrared- and Raman-active.

145 The mode which predicts a group theory for a pyramidal symmetry and the calculated phonon
 146 frequencies at the $\Gamma_{tot}(C_{3v})$ -point are reported in Table 2. They are attributed as shown in Table 2
 147 below in accordance with the assignments of the SbI₃ molecular vibrations [17]. The IR band
 148 attributions given here can be further substantiated by comparing of the
 149

150 **Table 2. Normal vibrational modes of the SbI₃ and SbTe₃ pyramids.**

151 **From the spectrum of a Ge-Sb-Te alloy composition Ge₁₅Sb₁₅Te₇₀.**

substance	Normal vibrational mode (cm ⁻¹) ^a						v3/v1	v4/v2
	v1	v2	v3	v4	vR	vT		
SbI ₃	177	89	147	71	67,5	45,5	0.83	0.80
SbTe ₃	164	122	145	106	53	46	0.88	0.86
Ge ₁₅ Sb ₁₅ Te ₇₀	157	127	142	109	56	45	0.90	0.87

152 v1 and v3 – the stretching modes for symmetric and antisymmetric vibrations,
 153 respectively;
 154 v2 and v4 – bending modes for symmetric and antisymmetric vibrations,
 155 respectively;
 156 vR and vT- external modes for pure rotation and pure translation, respectively.

157 ratio of the experimental frequencies of the stretching modes (ν_3/ν_1) and of the bending (ν_4/ν_2)
 158 modes for SbI_3 with similar values obtained in calculating the phonon modes for SbTe_3 . The important
 159 aspect of this comparison is that the frequency ratio ν_3/ν_1 and ν_4/ν_2 is essentially the same for the
 160 SbI_3 and for the SbTe_3 .

161 The calculated assignments of the IR bands in the spectrum of the crystalline $\text{Ge}_{15}\text{Sb}_{15}\text{Te}_{70}$
 162 presented in the Tables 1 and 2 are qualitatively comparable with assignment Raman frequencies of
 163 GST materials, reported in literature [18, 19]. So, main Raman bands peaking at 127 cm^{-1} and 157
 164 cm^{-1} in cubic $\text{Ge}_{22}\text{Sb}_{22}\text{Te}_{56}$ were also connected with stretch modes of GeTe_4 tetrahedra and SbTe_3
 165 pyramids, respectively. Our theoretical calculations show that bands peaking at 127 cm^{-1} and 157 cm^{-1}
 166 have also a contribution of $\nu_2(\text{A}_{1u})$ and $\nu_3(\text{E}_u)$ modes of SbTe_3 , respectively. More low-frequency
 167 band, covering $85\text{--}115\text{ cm}^{-1}$ frequency region of the far-IR spectrum of $\text{Ge}_{15}\text{Sb}_{15}\text{Te}_{70}$, comparable on
 168 intensity with the peaks of stretching modes GeTe_4 and SbTe_3 and is formed at least from two
 169 overlapping bands at 92 cm^{-1} and 110 cm^{-1} . These peaks according to the calculations can be
 170 attributed to bending modes $\nu_2(\text{E})$ and $\nu_4(\text{E}_u)$ of the GeTe_4 tetrahedra and SbTe_3 pyramids,
 171 respectively. In the frequency range $180\text{--}330\text{ cm}^{-1}$ far-IR spectrum of crystalline $\text{Ge}_{15}\text{Sb}_{15}\text{Te}_{70}$ one
 172 can recognize at least four small bands with maxima at $\sim 214, 260, 300, \text{ and } 320\text{ cm}^{-1}$ (see Figure).
 173 The first of them near 214 cm^{-1} apparently can be assigned to $\nu_3(\text{F}_2)$ asymmetric stretching modes of
 174 GeTe_4 tetrahedra. An analogous feature was observed in Raman spectra of bulk crystalline GeTe ,
 175 which are isostructural to $\text{Ge}_{22}\text{Sb}_{22}\text{Te}_{56}$ [20]. The weak bands at 260 and 320 cm^{-1} are quite probably
 176 due to the so-called 2 - phonon vibrational absorption arisen from excitations of fundamental
 177 molecular stretching modes of GeTe_4 (at 127 cm^{-1}) and SbTe_3 (at 157 cm^{-1}), respectively; while
 178 absorption band near 300 cm^{-1} can be related to vibrations of Ge-Ge ethane-like clusters [21].

179 The proposed interpretation of the IR-spectrum of polycrystalline $\text{Ge}_{15}\text{Sb}_{15}\text{Te}_{70}$ can be used for the
 180 attribution of the absorption bands at $\nu > 80\text{ cm}^{-1}$ of the IR-spectrum of the same
 181 alloy in amorphous (glassy) state. Because experimental spectra of these states in range, where are
 182 manifested intramolecular modes of the structural units of $\text{Ge}_{15}\text{Sb}_{15}\text{Te}_{70}$, practically do not differ from
 183 each other. Except of the negligible red shift and changes in bands shape of the IR-spectrum
 184 polycrystalline $\text{Ge}_{15}\text{Sb}_{15}\text{Te}_{70}$ with respect to that of the amorphous state. Since, as a rule, the
 185 crystalline phase is more ordered than the amorphous one, this fact shows unusual similarity of the
 186 amorphous and crystalline structures $\text{Ge}_{15}\text{Sb}_{15}\text{Te}_{70}$ of short range order, assuming a rather similar
 187 degree of topological 'disordering' between these two forms. This means, at the phase transition from
 188 the crystal to the amorphous phase, basically the local structure of the building blocks (tetrahedra and
 189 pyramids) of $\text{Ge}_{15}\text{Sb}_{15}\text{Te}_{70}$ remains unchanged.

190 The same time, by inspection of Figure 1, it is easily seen that the amorphous to crystal transition is
 191 displayed in the IR- spectra of $\text{Ge}_{15}\text{Sb}_{15}\text{Te}_{70}$ through drastic changes at $\nu < 80\text{ cm}^{-1}$, where is
 192 manifested lattice absorption due to external librational and translational degrees of freedom of the
 193 structural units of crystal. In the IR-spectrum of polycrystalline $\text{Ge}_{15}\text{Sb}_{15}\text{Te}_{70}$ with the manifestation of
 194 the intermolecular librations and translations of tetrahedra and pyramids as a whole, is connected,
 195 according to the calculations, the presence of absorption peaks at $65, 56, \text{ and } 45\text{ cm}^{-1}$ (modes $\nu\text{R}(\text{F}_1)$,
 196 $\nu\text{T}(\text{F}_2)$ and $\nu\text{T}(\text{E})$, respectively). In the IR-spectrum glassy $\text{Ge}_{15}\text{Sb}_{15}\text{Te}_{70}$ in the same frequency range
 197 is only one of abnormally broad band with a maximum at $\sim 60\text{ cm}^{-1}$, in which not difficult to discern the
 198 well-known, and ubiquitously present for amorphous solids, band, i.e. the boson peak.

199 Boson peak is attributed to the disorder-induced absorption, which is a manifestation of a low energy
 200 vibrational excitations emerging from cancellation of the selection rules in an amorphous medium. The
 201 peak observed in the low-frequency spectra of glasses appeared to correspond to the peaks
 202 observed at low frequencies in region of acoustic phonons of
 203 corresponding crystals [22]. Its appearance in the low-frequency spectra of glasses at the phase
 204 transition indicates that in the absence of a long-range order a system of coupled harmonic oscillators
 205 of crystal became a system of disoriented oscillators which preserve only limited (on a scale of
 206 medium-range order) correlation of the intermolecular vibrational motions [23]. So, in some works
 207 boson peak is assigned to cooperative orientational motion (librations) of several molecular groups
 208 [24, 25].

209 That is, as upon comparison IR-spectra of polycrystalline and glassy materials in range, where are
 210 manifested *intramolecular modes* of the structural units of $\text{Ge}_{15}\text{Sb}_{15}\text{Te}_{70}$, we had no hint concerning
 211 the contrasting local structure between the amorphous and the crystalline phases, so and the
 212 appearance of the boson peak at frequencies of *intermolecular modes* allow suggest that and the
 213 medium-range crystalline order in glassy $\text{Ge}_{15}\text{Sb}_{15}\text{Te}_{70}$ are also stored. This data reflects clearly the
 214 local ordering of the atoms in the amorphous state which is similar to that in the crystalline
 215 $\text{Ge}_{15}\text{Sb}_{15}\text{Te}_{70}$ but lacks long-range ordering.

216 The spectral changes at low optical frequencies allow suggest the following scenario of a phase
 217 transition in the system $\text{Ge}_{15}\text{Sb}_{15}\text{Te}_{70}$. Local distortions inherent "tetrahedral" and "pyramidal"
 218 structural units of glassy $\text{Ge}_{15}\text{Sb}_{15}\text{Te}_{70}$, facilitating the formation of Ge-Ge and Ge-Sb bonds [26], and
 219 also correlated torsional oscillations (librations) of these structures, at the essential share of vacancy,
 220 form medium-range (chain-like) order in the system. The evidence of this is the presence of the boson
 221 peak in the spectrum. For the transition such a system in a metastable ordered not require
 222 restructuring of local structures, but rather reorientation of existing clusters (the chains). In essence,
 223 the transition of the order-disorder in this case is the relaxation transition on the mechanism of fast β -
 224 relaxation Johari-Goldstein [27]. Such a transition requires minimal power inputs and has a
 225 nanosecond time of relaxation.

226 227 **4. CONCLUSION**

228
229 In the present work the far-infrared transmission spectra of polycrystalline and glassy materials of the
 230 GST system of composition $\text{Ge}_{15}\text{Sb}_{15}\text{Te}_{70}$ have been obtained in the spectral range 20 - 400 cm^{-1} at
 231 room temperature and also analyzed on the basis of theoretical calculation and of the literature data.
 232 Although the made vibrational assignments of various absorption bands given here could be
 233 considered as tentative and alternative interpretations may be proposed, these assignments and the
 234 revealed differences in the spectra is allow suggest the following possible molecular mechanism for
 235 unusual amorphization- crystallization process in GST alloys.

236 According to the majority of existing models, the presence of the boson peak, as an indication of a
 237 medium-range order existing in the structure of glasses, in the low-frequency spectra is associated
 238 with the correlative orientational motion (librations) of fragments a crystalline structure of glass. These
 239 fragments of a crystalline structure can play the role of crystallization centers on the nanometer scale
 240 and their correlative librational vibrations can be viewed as precursors of phonons due to short-range
 241 ordering. Then according to this model, the recrystallization from the amorphous phase may be
 242 achieved easily by reorientation of the randomly oriented fragments of a crystalline structure back to
 243 the original well-aligned structure of the crystalline phase. We emphasize that in this case
 244 crystallization of GST does not involve relaxation of the complete covalent network but is more like the
 245 so- called β -relaxation, where only fragments of the network relax. This process requires very small
 246 atomic displacements and hence can be extremely fast.

247 248 **REFERENCES**

- 249
250 1. Kolobov AV, Tominaga J. Chalcogenides: Metastability and Phase Change Phenomena; Press:
 251 Springer-Verlag, Berlin; 2012.
 252 2. Meinders ER, Mijiritskii AV, van Pieterse L, Wuttig M. Optical Data Storage Phase-Change Media
 253 and Recording; Philips Research Book Series, V. 4. Press: Springer- Verlag, Berlin; 2006.
 254 3. Burr GF, Breitwisch MJ, Franceschini M. et al. Phase change memory technology. J. Vac. Sci.
 255 Technology B 2010; 28:223-262.
 256 4. Kolobov AV, Fons P, Frenkel AI, Ankudinov AL, Tominaga J, and Uruga T. Understanding the
 257 phase-change mechanism of rewritable optical media. Nature Materials. 2004;3(10): 703-708.
 258 5. Shportko K, Kremers S, Woda M, Lencer D, Robertson J, Wuttig M. Resonant
 259 bonding in crystalline phase-change materials. Nature Materials. 2008;7(8):653-658.
 260 6. Wuttig M, Lusebrink D, Wamwangi D, Welnic W, Gilleben M, Dronskowski R. The role of vacancies
 261 and local distortions in the design of new phase-change materials. Nature Materials. 2007; 6(2):122-
 262 128.
 263 7. Raty JY, Godlevsky V, Ghosez P, Bichara C, Gaspard JP, and Chelikowsky JR. Evidence of a
 264 Reentrant Peierls Distortion in Liquid GeTe. Phys. Rev. Lett. 2000; 85:1950 - 1953.
 265 8. Cai YF, P. Zhou P, Lin YY, Tang TA, Chen LY, Li J et al. Nitrogen and Silicon Co-Doping of
 266 $\text{Ge}_2\text{Sb}_2\text{Te}_5$ Thin Films for Improving Phase Change Memory Performance. Chin. Phys. Lett. 2007;
 267 24(3):781 - 783.
 268 9. Moller K, Rothshild W. Far Infrared Spectroscopy. Press: Wiley, New York; 1971.
 269 10. Martin AJ, and Brenig W. Model for Brillouin Scattering in Amorphous Solids. Phys. Status Solidi B
 270 1974; 64(1):163-172.
 271 11. Mendoza-Galvan A, and Gonzalez-Hernandez J. Drude-like behavior of Ge:Sb:Te alloys in the
 272 infrared. J. Appl. Physics. 2000; 87:760-765.
 273 12. Kadlec F, Kadlec C, Kuzel P. Contrast in terahertz conductivity of phase-change materials. Solid
 274 State Communications. 2012;152(10):852-855.

- 275 13. Dzhurkov V, Fefelov S, Arsova, Nesheva D, and Kazakova L. Electrical conductivity and optical
276 properties of tellurium-rich Ge-Sb-Te films. Journal of Physics: Conference Series. 2014;558:012046 -
277 1 - 6.
- 278 14. Herzberg G. Molecular Spectra and Molecular Structure. II. Infrared and Raman Spectra of
279 Polyatomic Molecules; Press: D. Van Nostrand, London; 1945.
- 280 15. Stammreich H, Forneris Roberto, and Tavares Yara. Raman Spectra and Force Constants of
281 GeI₄ and SnI₄. J. Chem. Phys. 1956;25:1278-1279.
- 282 16. Delwaulle ML. Mise en evidence par l'effet Raman de la formation de chlorobromiodures de
283 germanium lorsqu'on melange les tetrachlorure, tetrabromure et tetraiodure de germanium. C. R.
284 Acad. Sci. 1954; 238:84-87. French.
- 285 17. Kiefer W. Raman-Spektreneines AsJ₃-Einkristalls und von SbJ₃ - und BiJ₃ - Kristallpulvern. Z.
286 Naturforsch. 1970; 25a:1101-1107. Germany.
- 287 18. Nemec P, Nazabal V, Moreac A, Gutwirth J, Bene L, Frumar M. Amorphous and crystallized Ge-
288 Sb-Te thin films deposited by pulsed laser: Local structure using Raman scattering spectroscopy.
289 Materials Chemistry and Physics.2012; 136:935-941.
- 290 19. Kozyukhin S, Veres M, Nguyen HP, Ingramd A, Kudoyarova V. Structural changes in doped
291 Ge₂Sb₂Te₅ thin films studied by Raman spectroscopy.
292 Physics Procedia.2013; 44:82- 90.
- 293 20. Upadhyay M, Murugavel S, Anbarasu M, and Ravindran TR. Structural study on amorphous and
294 crystalline state of phase change material. J. Appl. Phys. 2011;110:083711 - 1 - 6.
- 295 21. Koblar J, Arlin B, Shau G, Porezag DV, and Pederson MR. Raman-active modes of a-GeSe₂ and
296 a-GeS₂ : A first-principles study. Phys. Rev. B 1999; 60:R14985 - R14989.
- 297 22. Grigera TS, Martin-Mayor V, Parisi G. & Verrocchio P. Phonon interpretation of the 'boson peak' in
298 supercooled liquids. Nature.2003; 422:289-292.
- 299 23. Johari GP. Molecular inertial effects in liquids: Poley absorption, collision-induced absorption, low-
300 frequency Raman spectrum and Boson peaks. J Non-Crystalline Solids. 2000; 307-310:114-127.
- 301 24. Bembenek SD, Laird BB. Instantaneous normal modes analysis of amorphous and supercooled
302 silica. J. Chem. Phys. 2001; 114:2340=2344.
- 303 25. Baran J, Davydova NA, Pietraszko A. Spectroscopic study of the formation of molecular glasses.
304 J. Molec. Structure. 2005; 744-747:301-305.
- 305 26. Kolobov AV, Krbal M, Fons P, Tominaga J, Uruga T. Distortion-triggered loss of long-range order
306 in solids with bonding energy hierarchy. Nature Chemistry.2011; 3:311 - 316.
- 307 27. Johari GP. Localized molecular motions of P-relaxation and its energy landscape.
308 J. Non-Crystalline Solids. 2002; 307-310:317-325.